Available online at www.sciencedirect.com
SCIENCE DIRECT®
Journal of Nuclear Materials 329–333 (2004) 742–746
journal of nuclear materials
www.elsevier.com/locate/jnucmat

Microscopic damage of materials exposed to glow discharge cleanings in LHD

M. Miyamoto [a,*], M. Tokitani [a], K. Tokunaga [b], T. Fujiwara [b], N. Yoshida [b], S. Masuzaki [c], A. Komori [c]

[a] *Interdisciplinary Graduate School of Engineering Science, Kyushu University, Kasuga, Fukuoka 816-8580, Japan*
[b] *Research Institute for Applied Mechanics, Kyushu University, Kasuga, Fukuoka 816-8580, Japan*
[c] *National Institute for Fusion Science, Oroshi, Toki, Gifu 509-5292, Japan*

Abstract

Helium glow discharge cleaning (He-GDC) is frequently applied to reduce impurities like oxygen on the plasma facing materials in many plasma confinement devices, including large helical device (LHD). However, there are few reports which evaluated the wall conditioning effect from the point of view of the microstructure of materials. In the present study, therefore, microscopic damage to metals exposed to He-GDC in LHD were examined. Large numbers of dislocation loops and very high density of bubbles with sizes of 2–20 nm were formed by exposing to He-GDC. In addition, impurity deposits composed of Fe and Cr, which seemed to be re-deposited after sputtering of the first wall (SUS316L), were formed on all specimens. These serious surface modifications seem to have a larger impact on plasma fuel recycling under main plasma discharges. Instead of restoring the wall, significant damage by He-GDC creates gas trapping sites.

1. Introduction

Helium glow discharge cleaning (He-GDC) is frequently applied to reduce impurities like oxygen on the plasma facing materials (PFMs) in many plasma confinement devices. Especially in devices with superconducting coils such as large helical device (LHD), GDC appears to be a convenient method for wall conditioning without recourse to baking at high temperatures. However, it is known that He-GDC can have harmful effects on controlling plasma density and on vacuum leak testing with He gas in some devices because of absorption of large amounts of He gas trapped in materials during He-GDC [1,2]. In addition, it is apparent that He atoms have strong effects on material damage even if they do not have sufficient energy for knock-on damage [3].

To investigate these issues, focused research on the interaction of He-GDC and materials in these devises is required. In the present study microscopic damage in metals exposed to He-GDC in LHD was evaluated and the impact on fuel recycling processes is discussed.

2. Experimental setup

LHD is a superconducting heliotron type device with a first wall made of stainless steel (SUS316L) and graphite divertor tiles [2,4]. The surface modifications caused by He-GDC were examined using a material probe experiment. Pre-thinned vacuum-annealed disks of 3 mm diameter made of poly-crystalline SUS316L, W (99.95%), Mo (99.95%) and Cu (99.9%) were used as specimens. The specimens mounted on the material probe system, which has the same electric potential as the vacuum vessel, were placed at a position similar to

* Corresponding author. Address: Department of Material Science, Interdisciplinary Faculty of Science and Engineering, Shimane University, 1060 Nishikawatsu, Matsue 690-8504, Japan. Tel.: +81-852 32 6448; fax: +81-852 32 6409.
E-mail address: miyamoto@riko.shimane-u.ac.jp (M. Miyamoto).

0022-3115/$ - see front matter © 2004 Elsevier B.V. All rights reserved.
doi:10.1016/j.jnucmat.2004.04.181

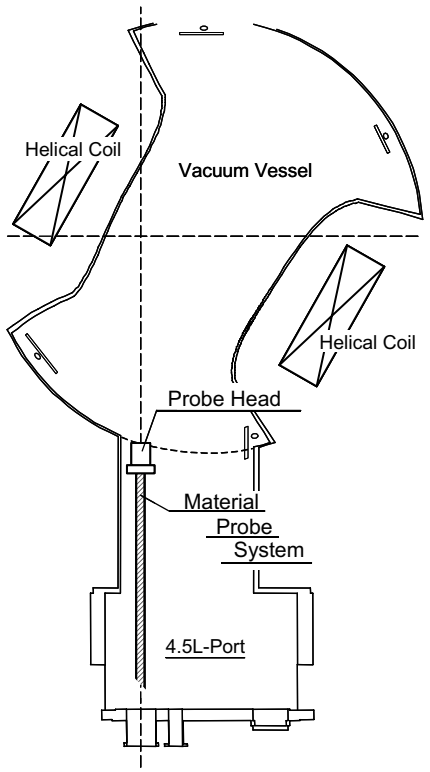

Fig. 1. Schematic view of the experimental set up in LHD.

the first wall surface through the 4.5 low port (4.5L) as shown in Fig. 1. He-GDC was carried out with two electrodes inserted into the vacuum vessel from the 4.5 upper port (4.5U) and 10.5U. The voltage, electric current and duration time were 200 V, 20 A and 65 h, respectively, hence fluence was roughly estimated at 3.7×10^{22} He/m^2 by using the total plasma facing surface area of 780 m^2. The temperature of the specimen holder during He-GDC stayed almost constant at room temperature.

After exposing to He-GDC, the microstructure of specimens was observed by means of transmission electron microscopy (TEM) and atomic force microscopy (AFM). Chemical composition of impurity deposition formed on specimens was examined by energy dispersive spectroscopy (EDS) equipped on the TEM.

For further information on damage, irradiation experiments on SUS316L were also carried out at room temperature using bombardment with 2 keV He ions.

3. Results

3.1. Microstructures

After exposing the specimens to He-GDC, their microstructures were remarkably changed. Fig. 2 shows a typical microstructure of the SUS316L specimen after the exposure to He-GDC. A large hole of about 100–200 nm in diameter appeared on the pre-thinned specimen and a high density of bubbles (white image) with sizes 2–20 nm was also formed. Surface morphology obtained by AFM observation of the SUS316L specimen after the exposure is shown in Fig. 3. The irradiated surface is covered by depressions which seemed to be formed by exfoliation of fine blisters. This heavy damage such as the large hole had not been observed in irradiation experiments with helium ions of 2 keV, as shown in Fig. 2. In the case of the He ion irradiation experiment, only the fine bubbles with size of about 2 nm were observed.

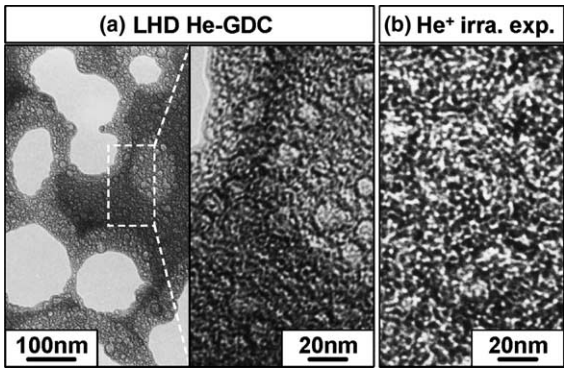

Fig. 2. Microstructure of SUS316L exposed to He-GDC (a) and irradiated with 2 keV-He$^+$ at room temperature to a fluence of 1×10^{22} He/m^2 (b).

The depth distribution of He bubbles formed in SUS316L exposed He-GDC is plotted in Fig. 4 together with the injected He atom distribution calculated by TRIM91-code for 200 eV-He$^+$. The data for irradiation experiments with 2 keV-He$^+$ are also plotted in the figure for comparison. In the case of He-GDC, the He bubbles are distributed to quite a deep range, well

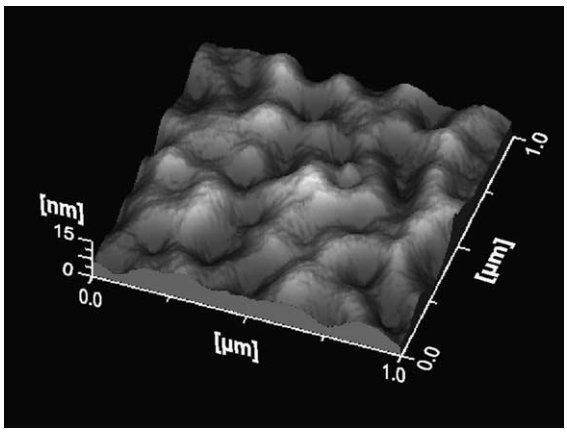

Fig. 3. Surface morphology of SUS316L exposed to He-GDC.

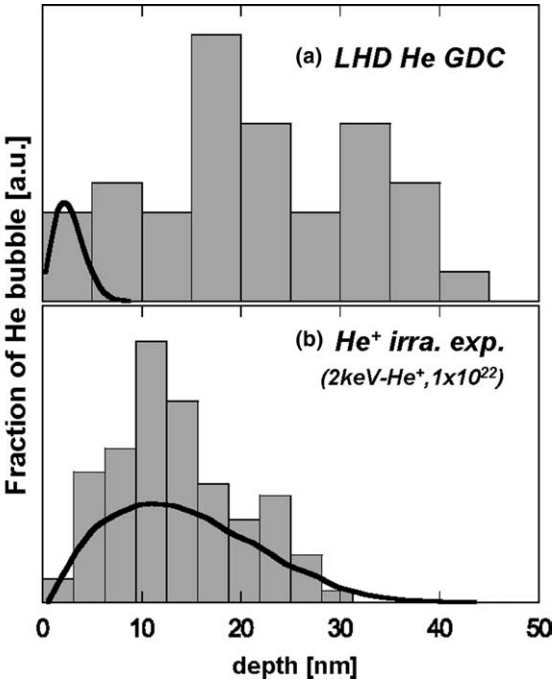

Fig. 4. Depth distribution of He-bubbles formed in SUS316L exposed to He-GDC (a) and irradiated with 2 keV He^+ at room temperature to a fluence of 1×10^{22} He/m^2 (b). Calculated injected He atom profiles are compared.

beyond the injected range. This is in contrast to the irradiation experiment case, where the He bubble distribution is approximately the same as the injected range. This indicates that many of the He atoms in the He-GDC case had diffused deeper into the material, even though the injected energy is rather low.

Similar heavy damage was observed in all specimens examined. Fig. 5 shows microstructures in SUS316L, Mo, W and Cu. The circular white contrast in bright field images at large deviation parameter condition (top figures) and sharp white dot contrast in dark field images (bottom figures) are He bubbles and dislocation loops, respectively. In all specimens, both a high density of bubbles and also dislocation loops were formed by the exposure. One should note that the heavy damage formed even in W which does not experience knock-on damage by irradiation with 200 eV-He^+.

3.2. Impurity deposition

In addition to the large amount of damage described above, impurity deposits were also identified on all specimens exposed to the He-GDC. Fig. 6 shows the dark field images and the corresponding electron diffraction pattern of the SUS316L specimen. The images were obtained from a part of the first broad diffraction ring. Under this imaging condition, only the crystal grains satisfying the Bragg condition show up in white

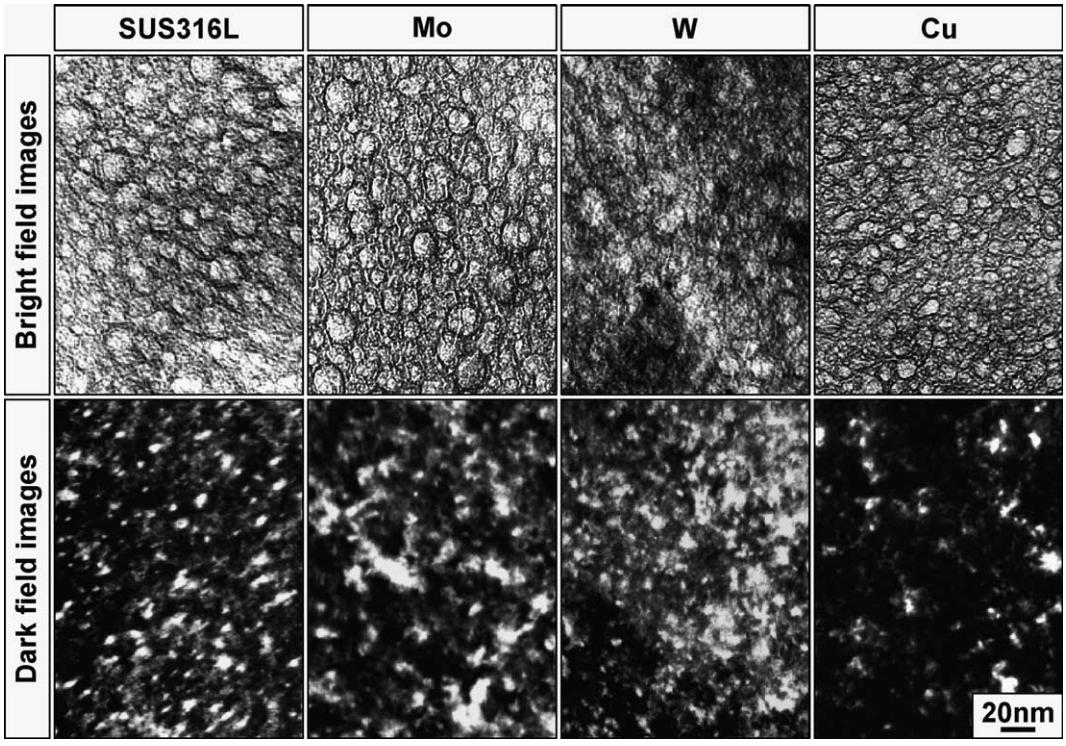

Fig. 5. Microstructure of several specimens exposed to He-GDC.

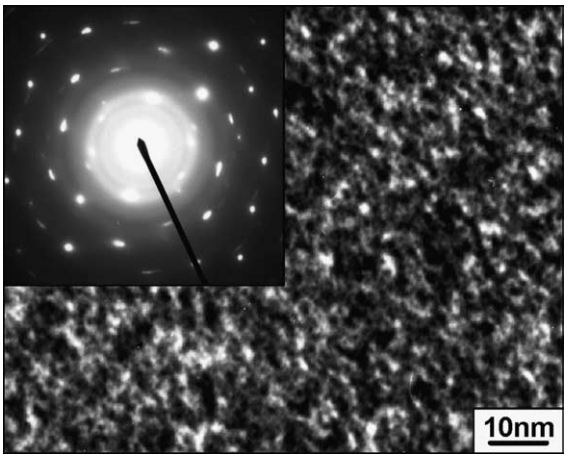

Fig. 6. Electron diffraction pattern and microstructure of the impurity deposits formed on SUS316L exposed to He-GDC. Images with white contrast show individual grains.

contrast. The numerous small dot contrasts indicate that the formation of impurities deposition consisted of fine grains only 1–2 nm in diameter. The radius and intensity of the diffraction rings show that the impurity deposits had a similar crystal structure to stainless steel, that is, fcc structure and the lattice constant of 0.39 nm. Moreover, Fe and Cr were detected as deposition elements by the EDS measurement. These results indicate that the impurities originated from sputtering of the first wall (SUS316L) that re-deposited onto the specimens.

4. Discussion

Because the threshold energy of He ions for displacement damage in W and Mo are about 0.53 and 0.23 keV, respectively, direct formation of vacancies and interstitial atoms by a knock-on process is not expected in the present LHD experiment. In addition, since the energy of most He atoms injected by He-GDC is less than 0.2 keV, little of no damage is expected even in SUS316L which has a threshold energy of 0.1 keV. However, significant defect formation occurred in these specimens exposed to the He-GDC as shown in Fig. 5. These defects formed without knock-on processes are a characteristic feature of He irradiation and have been also observed in He ions and He plasma irradiation experiments [3,5]. It should be noted that He inflicts very strong damage even at low energy such as in the He-GDC case.

The difference in the depth distribution of He bubbles is shown clearly in Fig. 4. This difference seems to be the result of the concentration of vacancies formed by knock-on process. In the case of 2 keV-He^+ irradiation, radiation induced numerous vacancies that serve as trapping sites for injected He atoms and thus hinder the diffusion of He atoms. As a result, He bubbles are limited to within the injected depth ranges. On the other hand, because knock-on damage is not created by He-GDC, injected He atoms can diffuse easily, and the peak depth of the distribution is shifted toward much deeper regions as compared to the injected range. This indicates that He-GDC brings about the widespread damage rather than restoring a material surface. It is believed that the high mobility of He through interstitial sites and large reduction of internal energy by agglomeration result in the easy formation of this unexpected damage.

In addition, the surface sputtering, which is calculated to be about 18 nm erosion, exposes the heavily damaged region. Thus, the material surface becomes covered with many fine blisters and dense bubbles. This indicates the increase of the surface area of the materials. Unfortunately, this enlarged surface area may make vacuum properties worse by the adsorption of a large quantity of impurity gases. It is also likely that these damaged sub-surface regions act as sources of He outgassing. As the authors reported [6], irradiation experiments with fluences above the order of 10^{21} He/m^2 on SUS316L showed that significant desorption of He occurred even at room temperature.

The effects of He ion irradiation on trapping of injected hydrogen isotopes in many metals have been studied [7–9]. According to these references, pre-damage by He ions produces a significant concentration of hydrogen isotope trapping sites. Furthermore, the effect of impurity deposition on the hydrogen isotope recycling process cannot be overlooked. Hino et al. [10] have reported the formation of metallic impurities deposits including a large amount of oxygen in their material probe experiments in LHD. When the co-deposition of metal and oxygen is formed, it is known that the deposit has a peculiar defect structure consisted of fine grains [11], which is similar to the deposits observed in this study. The deposition shown in Fig. 5 is thus estimated to also include oxygen. If co-deposition of metallic impurities and oxygen occurs, the deposited layer has very strong trapping potential for hydrogen isotope even in metallic materials, which are known to have low retention without the included oxygen [12].

According to the discussion above, the total amount of retained hydrogen isotopes increases drastically with the surface modifications caused by the He-GDC. This effect seems to decrease the fuel recycling coefficient of the wall in the case of the main plasma discharge experiments with a short pulse, with the wall acting as if it were refreshed. However, in the case of long-pulse discharges, these retained hydrogen isotopes will be desorbed occasionally, and plasma density control will be difficult.

From the point of view of material damage, it can be said that the He-GDC of the metal wall is just a

temporary solution to get out of a present difficulty. Now, the perfect conditioning method, which satisfies all needs, is not yet devised. Because the heavy wall damage observed in this study originates from the characteristic features of He atoms in metals, easy migration through lattice and strong aggregation, GDC with different gases needs to be invested. Candidates such as Ne and Ar might have different feature in metals. Furthermore, in order to optimize wall conditioning methods, other methods and their combined effects should be examined.

5. Summary

The material probe experiment was carried out by exposing specimens to the He-GDC in LHD. A large concentration of dislocation loops and very dense bubbles were formed in the specimens, with broad distributions beyond the injected range. In addition, impurities that originated from sputtering of the first wall were re-deposited on the specimens. This damage and the deposits drastically enhance hydrogen isotopes trapping capability. It follows that the effect of He-GDC on wall exhaust capability being recovered depends on the strong trapping effects of heavily damaged materials. From the point of view of material damage, it can be said that the He-GDC for the metal wall is just a temporary solution to get out of a present difficulty.

References

[1] D. Tafalla, F.L. Tabares, J. Nucl. Mater. 290–293 (2001) 1195.
[2] H. Suzuki et al., J. Nucl. Mater. 313–316 (2003) 297.
[3] H. Iwakiri et al., J. Nucl. Mater. 283–287 (2000) 1134.
[4] S. Masuzaki et al., J. Nucl. Mater. 290–293 (2001) 12.
[5] N. Yoshida et al., Nucl. Fusion 43 (2003) 655.
[6] M. Tokitani et al., J. Nucl. Mater., these Proceedings. doi:10.1016/j.jnucmat.2004.04.177.
[7] A.E. Pontau et al., J. Nucl. Mater. 111&112 (1982) 651.
[8] H. Iwakiri et al., J. Nucl. Mater. 307–311 (2002) 135.
[9] S.T. Picraux et al., Appl. Phys. Lett. 28 (1976) 179.
[10] T. Hino et al., J. Nucl. Mater. 290–293 (2001) 1176.
[11] T. Hirai et al., J. Nucl. Mater. 283–287 (2000) 1177.
[12] M. Miyamoto et al., J. Nucl. Mater. 313–316 (2003) 82.